JOURNAL OF VIROLOGY, Aug. 2011, p. 7775–7787 Vol. 85, No. 15
0022-538X/11/$12.00 doi:10.1128/JVI.00665-11

A Single Amino Acid in Nonstructural Protein NS4B Confers Virulence to Dengue Virus in AG129 Mice through Enhancement of Viral RNA Synthesis▽†

Dixon Grant,[1,2]‡ Grace K. Tan,[3]‡ Min Qing,[1,4]‡ Jowin K. W. Ng,[3] Andy Yip,[1] Gang Zou,[1] Xuping Xie,[1,4] Zhiming Yuan,[4] Mark J. Schreiber,[1] Wouter Schul,[1]§ Pei-Yong Shi,[1]§* and Sylvie Alonso[3]§*

Novartis Institute for Tropical Diseases,[1] Duke-National University of Singapore Graduate Medical School,[2] and Department of Microbiology, Immunology Programme, National University of Singapore,[3] Singapore, and State Key Laboratory of Virology, Wuhan Institute of Virology, Chinese Academy of Science, China[4]

Received 2 April 2011/Accepted 14 May 2011

Dengue (DEN) is a mosquito-borne viral disease that has become an increasing economic and health burden for the tropical and subtropical world. The lack of an appropriate animal model of DEN has greatly impeded the study of its pathogenesis and the development of vaccines/antivirals. We recently reported a DEN virus 2 (DENV-2) strain (D2Y98P) that lethally infects immunocompromised AG129 mice, resulting in organ damage or dysfunction and increased vascular permeability, hallmarks of severe DEN in patients (G. K. Tan et al., PLoS Negl. Trop. Dis. 4:e672, 2010). Here we report the identification of one critical virulence determinant of strain D2Y98P. By mutagenesis, we showed that a Phe-to-Leu alteration at amino acid position 52 in nonstructural protein NS4B completely abolished the pathogenicity of the D2Y98P virus, as evidenced by a lack of lethality and the absence of histological signs of disease, which correlated with reduced viral titers and intact vascular permeability. Conversely, a Leu-to-Phe alteration at position 52 of NS4B in nonvirulent DENV-2 strain TSV01 led to 80% lethality and increased viremia. The NS4B(Phe52) viruses displayed enhanced RNA synthesis in mammalian cells but not in mosquito cells. The increased viral RNA synthesis was independent of the ability of NS4B to interfere with the host type I interferon response. Overall, our results demonstrate that Phe at position 52 in NS4B confers virulence in mice on two independent DENV-2 strains through enhancement of viral RNA synthesis. In addition to providing further insights into the functional role of NS4B protein, our findings further support a direct relationship between viral loads and DEN pathogenesis *in vivo*, consistent with observations in DEN patients.

Dengue (DEN) disease, caused by any one of the four serotypes of dengue virus (DENV), is a major global public health and economic burden. DENV affects 2.5 billion people worldwide, mostly in tropical and subtropical countries, leading to 50 to 100 million human infections each year (13). Clinical manifestations of DEN disease range from undifferentiated fever to DEN fever (DF) and DEN hemorrhagic fever (DHF), with plasma leakage that may lead to hypovolemic shock (DEN shock syndrome [DSS]). Therapeutic intervention is limited to fluid management for DEN patients who experience severe vascular leakage (41). Currently, no antiviral therapy or vaccine to fight DEN is available on the market (9, 31).

DENV belongs to the genus *Flavivirus* within the family *Flaviviridae*. Besides DENV, many other flaviviruses are important human pathogens, including yellow fever virus (YFV), West Nile virus (WNV), Japanese encephalitis virus (JEV), and tick-borne encephalitis virus (TBEV). DENV is a small enveloped virus with a positive single-strand RNA of approximately 10,700 nucleotides (18). The DENV genome encodes 10 proteins, comprising 3 structural proteins (capsid [C], premembrane [PrM], and envelope [E]) and 7 nonstructural proteins (NS1, NS2A, NS2B, NS3, NS4A, NS4B, and NS5). The structural proteins form the viral particle. The nonstructural proteins participate in RNA replication, virion assembly, and evasion of innate immune responses (24). Limited data on the functional role of NS4B are available. Previous studies have indicated that NS4B and, to a lesser extent, NS2A and NS4A block type I interferon (IFN) signaling (12, 25, 29, 30). NS5 also antagonizes type I IFN signaling (4, 19) and mediates STAT2 degradation (1).

The mechanisms involved in DEN pathogenesis have yet to be fully understood and result from a complex interplay between viral and host factors. In the host, immune status, age, sex, and genetic factors may contribute to disease severity. Numerous field studies have indicated a link between disease severity and the DENV genome sequence (2, 3, 22, 27, 38). A number of viral determinants modulating the intrinsic virulence of the virus within its host have been identified and have been shown to affect either the binding properties (7, 11, 33, 37) or the replication efficiency (20, 34) of DENV. Such knowledge has proven useful for the development of live attenuated

* Corresponding author. Mailing address for Sylvie Alonso: CeLS Building, 28 Medical Drive, Singapore 117597. Phone: 65 6516 3541. Fax: 65 6778 2684. E-mail: micas@nus.edu.sg. Mailing address for Pei-Yong Shi: Novartis Institute for Tropical Diseases, 10 Biopolis Rd., Singapore 138670. Phone: 65 6722 2909. Fax: 65 6722 2916. E-mail: pei_yong.shi@novartis.com.

† Supplemental material for this article may be found at http://jvi.asm.org/.

‡ D.G., G.K.T., and M. Q. made equal contributions to the study.

§ W.S., P.-Y.S., and S.A. are co-senior authors of the paper.

▽ Published ahead of print on 1 June 2011.

DENV vaccine candidates (10, 17, 46). A number of animal models have been reported that partially reproduce some of the clinical features of human DEN disease, such as hemorrhage or increased vascular permeability (16). However, no animal model that mimics the disease progression and recapitulates a number of clinical manifestations is available yet, and the lack of such a model has impeded the dengue pathogenesis research field and the development of effective vaccines and antivirals. We recently reported a non-mouse-adapted DENV-2 strain (D2Y98P) that can lethally infect AG129 mice (with the alpha/beta interferon [IFN-α/β] and IFN-γ receptors knocked out) (39). Infection with D2Y98P led to transient viral replication in the blood and several organs (including the spleen, liver, and intestine) that resulted in severe organ damage and increased vascular permeability.

In this study, we investigated the viral determinant(s) that contributes to the virulence of strain D2Y98P in AG129 mice. We demonstrate that a single amino acid substitution at position 52 (F52L) in the NS4B protein abolishes D2Y98P virulence in mice. Conversely, an L52F substitution conferred virulence on strain TSV01, a nonvirulent DENV-2 strain unrelated to D2Y98P. Mechanistically, we showed that Phe at position 52 in NS4B protein enhanced viral RNA synthesis in mammalian cells and that this mechanism is independent of the protein's ability to interfere with the host type I IFN response. Our work thus highlights the importance of NS4B protein during DENV replication and demonstrates a correlation between viral replication efficiency, viral loads, and virulence in AG129 mice, as proposed for DEN patients.

MATERIALS AND METHODS

Ethics statement. All the animal experiments were carried out under the guidelines and upon the approval of the animal ethics committees of the National University of Singapore (NUS) and Novartis Institute for Tropical Diseases (NITD). The blood withdrawal procedure was performed under anesthesia, and all efforts were made to minimize suffering.

Cells and viruses. Vero, BHK-21, A549, 293T, and C6/36 cells were obtained from the American Type Culture Collection (ATCC). 293T cells were cultured in minimal essential medium (MEM) containing 10% fetal bovine serum (FBS) and 0.1 mM nonessential amino acids. Vero cells (a monkey kidney epithelial cell line) and BHK-21 cells (a baby hamster kidney cell line) were maintained in Dulbecco's modified Eagle medium (DMEM) containing 10% FBS, and virus infection was performed in DMEM plus 2% FBS. A549 cells (a human pulmonary epithelial cell line) were maintained in F-12 medium plus 10% FBS, and virus infection was performed in F-12 medium plus 2% FBS. C6/36 cells (an *Aedes albopictus* cell line) were cultured in RPMI 1640 medium with 10% FBS, and virus infection was performed in RPMI 1640 medium with 5% FBS.

DENV-2 strain D2Y98P was isolated from a DEN patient in Singapore in 1998 and has been passaged in C6/36 cells for approximately 20 rounds (39). D2Y98P was plaque purified twice sequentially on BHK-21 cells, yielding the D2Y98P-PP1 virus strain, whose genome has been fully sequenced (GenBank accession number JF327392). D2MY00-22563 (GenBank accession number FN429892) is a DENV-2 clinical isolate recovered in Malaysia in 2000 and obtained as a kind gift from Shamala Devi (Department of Medical Microbiology, University of Malaya, Kuala Lumpur, Malaysia). DENV-2 strain TSV01 was derived from an infectious cDNA clone (35). All viruses were stored at −80°C.

Plaque assay. Plaque assays were carried out in BHK-21 cells as described previously (39). Briefly, 2×10^5 BHK-21 cells were seeded in 24-well plates (Nunc, NY). The virus stock was 10-fold serially diluted from 10^{-1} to 10^{-6} in RPMI 1640 (GIBCO). BHK-21 monolayers were infected with 100 μl of each virus dilution. After incubation at 37°C under a 5% CO_2 atmosphere for 1 h with rocking at 15-min intervals, the medium was decanted, and 0.6 ml of 0.8% (wt/vol) carboxymethyl cellulose in RPMI medium supplemented with 2% FCS was added to each well. After 4 days of incubation at 37°C under 5% CO_2, the cells were fixed with 4% paraformaldehyde and were stained for 30 min with 200 μl of 1% crystal violet dissolved in 37% formaldehyde. After thorough rinsing with water, the plates were dried; the plaques were scored visually; and the score was expressed as the number of PFU. Triplicate wells were run for each dilution of each sample. The limit of detection for the plaque assay is set at 10 PFU per milliliter or per gram of tissue.

Plaque purification. Two rounds of plaque purification of the D2Y98P virus suspension were performed in 6-well plates seeded with 1×10^6 BHK-21 cells. The virus was serially diluted from 10^2 to 10^6 PFU/ml; 200 μl of virus was added; and plates were incubated with shaking for 1 h. The virus was removed, and 2 ml of the first overlay (1.7 ml of 7.5% $NaHCO_3$, 2 ml of 1% [wt/vol] DEAE dextran, 50 ml of 2× basal medium Eagle [BME] with 2% [vol/vol] FBS, and 50 ml of 1.2% [wt/vol] Oxoid agar) was added. Plates were incubated at 37°C under 5% CO_2. Three to 5 days later, 2 ml of the second overlay (consisting of the recipe given above with 50 ml of 2% [wt/vol] Noble agar in place of the Oxoid agar and 1.2 ml of 0.3% neutral red stain) was added. Individual plaques were picked and amplified in 24-well plates seeded with 2×10^5 BHK-21 cells in 500 μl of growth medium. The plaque purification process described above was repeated once. The double-purified virus suspension, named D2Y98P-PP1, was amplified in C6/36 cells and was quantified by a plaque assay as described above.

Quantification of viral particles from cell cultures. Mammalian or mosquito cell monolayers in T25 flasks were infected with different DENV strains at the multiplicities of infection (MOI) indicated in the figure legends. At different time points postinfection (p.i.), the supernatants were harvested, and the cell monolayers were washed in phosphate-buffered saline (PBS), incubated for 3 min on ice with an alkaline high-salt solution of 1 M NaCl plus 50 mM Na bicarbonate (pH 9.5) to remove surface-bound virus, and washed two more times in PBS. Cells were then trypsinized from the flask to ensure that all the cells were collected before undergoing lysis via freeze-thaw cycles (15). Virus titers in the cell lysates were measured by plaque assays as described above.

Extraction of viral RNA from infected cells and RT-PCR. Viral RNA was extracted from the cell lysates using an RNeasy Mini kit (Qiagen) according to the manufacturer's instructions. Purified RNA was treated using the RNase-free DNase set (Qiagen) to remove contaminant DNA. Reverse transcription was performed on 10 ng of total RNA using the iScript cDNA synthesis kit (Bio-Rad Laboratories). Real-time PCR (RT-PCR) was performed in a 96-well plate in which each well contained 2 μl of cDNA, 0.5 μl of specific primers (final concentration, 0.5 μM), 22 μl H_2O, and 25 μl SYBR green SuperMix with ROX (Bio-Rad Laboratories). Samples were run in triplicate. RT-PCR amplification was conducted with the ABI Prism 7500 sequence detector (Perkin-Elmer Applied Biosystems) over 40 cycles with an annealing temperature of 60°C. Assessment of the expression of each target gene was based on relative quantification (RQ) using the comparative critical threshold (C_T) value method. The relative quantification of a specific gene was evaluated in each reaction by normalization to the C_T obtained for the endogenous control gene (the β-actin gene) from each respective cell line. RQ values were calculated by dividing the normalized C_T value obtained for each sample by the normalized C_T value obtained for the D2MY00-22563 sample at day 1 p.i. RQ values thus reflect the fold changes in the quantity of viral RNA relative to the quantity in the D2MY00-22563 sample at day 1 p.i. Control reactions without cDNA were used as negative controls. At least two independent experiments were conducted. The following primers were used: NS4B forward primer (FP), 5′-AACGgAgATgggTTTCCTggAA-3′; NS4B reverse primer (RP), 5′-TTCAAACTTTggATCATAgggT-3′; BHK-21 (β-actin) FP, 5′-AgAgggAAATTgTgCgTgAC-3′; BHK-21 (β-actin) RP, 5′-CAATggTgA TgACCTggCCA-3′; Vero (β-actin) FP, 5′-AgCgggAATCgTgCgTgAC-3′; Vero (β-actin) RP, 5′-CAATggTgATgACCTggCCA-3′; C6/36 (β-actin) FP, 5′-AAC gTgAAATCgTTCgTgAC-3′; C6/36 (β-actin) RP, 5′-CgATggTgATgACCTgTC Cg-3′.

Plasmid constructs. An infectious cDNA clone of the D2Y98P-PP1 virus was constructed by separating the viral genome into four subclones, followed by full-length cDNA assembly. Viral RNA was extracted from the D2Y98P-PP1 virus stock using the QIAamp Viral RNA Mini kit (Qiagen). The genomic RNA was used as a template for all RT-PCRs (Invitrogen). Figure S1 in the supplemental material summarizes the cloning strategy and nucleotide positions of each subclone used to produce fragments A to D. Fragment A was cloned into the low-copy-number vector pACYC177 (New England Biolabs), yielding recombinant plasmid pACYC-A, and contained an NheI restriction site, a T7 promoter sequence, and the first 1,850 nucleotides (with the BsrGI restriction site at nucleotide 1841, as indicated in Fig. S1) of the viral genome, followed by a nonviral XhoI restriction site (for cloning convenience). Fragments B, C, and D were cloned into the Topo TA vector (Invitrogen), yielding plasmids pCR2.1-B, pCR2.1-C, and pCR2.1-D, respectively. A hepatitis delta virus ribozyme (HDVr) sequence was added to the 3′ end of fragment D. Fragment B

was subcloned into pACYC-A, yielding plasmid pACYC-AB. Fragment C was cloned into pCR2.1-D, resulting in plasmid pCR2.1-CD. Finally, fragment CD was assembled into pACYC-AB, resulting in pACYC FL-D2Y98P-PP1. All the cloning steps were performed using Top10 One Shot chemically competent *Escherichia coli* cells (Invitrogen). Transformed *E. coli* cells were grown on LB agar plates or in LB broth containing 75 μg/ml ampicillin at 37°C. All subclones, as well as the full-length cDNA clone, were sequenced to ensure the absence of mutations.

The full-length DENV-2 TSV01 cDNA clone and a *Renilla* luciferase (Rluc) replicon cDNA clone have been described previously (35). The NS4B L52F substitution in the infectious TSV01 clone was engineered into shuttle vector B (35) using a QuikChange II XL site-directed mutagenesis kit (Stratagene). The mutant NS4B(L52F) DNA fragment was reintroduced into plasmid pFLTSV01 and the TSV01 replicon cDNA plasmid at the XhoI (nucleotide position 5426) and ClaI (located immediately downstream of the 3′ end of viral cDNA) sites.

IFN reporter assay. To analyze whether mutation of NS4B affected its antagonism of the IFN response, the genes encoding NS4B(L52) and NS4B(F52) were individually cloned into the mammalian expression vector pXJ. A hemagglutinin (HA) tag was fused to the 3′ ends of the genes to generate C-terminally HA-tagged NS4B(L52) and NS4B(F52) proteins. A reporter plasmid, pISRE-Luc (Clontech), containing an IFN-stimulated response element (ISRE) driving the expression of firefly luciferase (Luc), was used to quantify IFN-induced activation. phRLuc-TK (Promega), encoding *Renilla* luciferase under the control of the herpes simplex virus (HSV) thymidine kinase promoter, was used as an internal control for transfection efficiency. For quantification of the IFN response, 2×10^5 293T cells were transfected using the FuGENE HD transfection reagent (Roche) in a 24-well plate. Western blotting was carried out to check the expression of the HA-tagged proteins using anti-HA and anti-tubulin primary antibodies. The cells were cotransfected with three plasmids: 1 μg of a plasmid expressing NS4B(L52)-HA, NS4B(F52)-HA, or an empty vector; 0.3 μg of the pISRE-Luc plasmid; and 4 ng of the phRLuc-TK plasmid. At 24 h posttransfection, cells were incubated with 1,000 U/ml of human IFN-β (Sigma). After the cells were maintained in DMEM–10% FBS for another 24 h, they were assayed for both firefly and R luc activities using a Dual-Luciferase reporter assay system (Promega).

Immunofluorescence assay. A total of 4×10^5 BHK-21 cells were transfected with 0.5 μg of a plasmid expressing NS4B(L52)-HA, NS4B(F52)-HA, or an empty vector in an 8-chamber slide (Lab-Tek). At 24 h posttransfection, cells were incubated with human IFN-α (500 U/ml; Millipore Chemicon) for 30 min. After three washes with PBS, the cells were fixed in formaldehyde for 15 min at room temperature. Cell nuclei were permeabilized for 10 min in methanol at −20°C. A mouse monoclonal antibody against the HA probe (Santa Cruz Biotechnology) and a rabbit polyclonal antibody against phosphorylated STAT1 (Tyr-701) (Cell Signaling Technology) were used as primary antibodies. An Alexa Fluor 488 (green)-conjugated anti-mouse antibody and an Alexa Fluor 594 (red)-conjugated anti-rabbit antibody (Invitrogen) were used as secondary antibodies. Nuclei were stained with 4′,6-diamidino-2-phenylindole (DAPI) (Vectashield Mounting Medium with DAPI; Vector Laboratories). The cells were analyzed using a fluorescence microscope (Leica).

Transient replicon assay. Luciferase-reporting replicon RNA (10 μg) of strain TSV01 was electroporated into 8×10^6 BHK-21, A549, Vero, or C6/36 cells. Electroporation was performed at 25 μF and 850 V (BHK-21 cells) or 450 V (A549, Vero, and C6/36 cells) with three pulses at 3-s intervals. The cells were seeded in 12-well plates (4×10^5 cells per well). At various time points, the cells were washed once with cold PBS, and 200 μl of lysis buffer (Promega) was added. The plates containing the lysis buffer were sealed with Parafilm and were stored at −80°C. Once samples had been collected for all time points, 20-μl portions of the cell lysates were transferred to a 96-well plate and were assayed for luciferase signals in a Clarity luminescence microplate reader (BioTek).

Infection of mice. AG129 mice (129/Sv mice deficient in both the IFN-α/β and IFN-γ receptors) were obtained from B&K Universal (United Kingdom). They were housed under specific-pathogen-free conditions in individual ventilated cages. Eight- to 9-week-old mice were administered 10^6 PFU of the different DENV strains via the intraperitoneal (i.p.) route (0.4 ml in sterile PBS). The survival rate was derived from the number of mice that were euthanized at the moribund stage, evidenced by severe diarrhea, lethargy, and dramatic body weight loss, as described previously (39).

Determination of virus titers in infected mice. Blood samples were collected from the cheek vein in 0.4% sodium citrate and were centrifuged for 5 min at $6{,}000 \times g$ to obtain plasma. The presence of infectious viral particles was determined by a plaque assay as described above.

The levels of infectious virus in tissues from infected mice were assessed as described previously (39). Briefly, the animals were euthanized and were perfused systemically with sterile PBS. Whole tissues from the liver, the spleen, the brain, the spinal cord, the kidney, the skin of the back, the intestines, and the lungs were harvested from individual mice and were homogenized. Ten-fold serial dilutions of each homogenate (from the undiluted homogenate to a $1{:}10^5$ dilution) were assayed in a standard virus plaque assay on BHK-21 cells as described above. Triplicate wells were run for each dilution of each sample. Data are expressed as $\log_{10}$ PFU per gram of wet tissue (mean ± standard deviation [SD]), with the limit of sensitivity set at 1.0 $\log_{10}$ PFU/g of tissue. Five mice per time point per group were assessed. Results are representative of at least two independent experiments.

Histology. Mice were euthanized, and tissues were harvested and immediately fixed in 10% formalin in PBS. Fixed tissues were paraffin embedded, sectioned, and stained with hematoxylin and eosin (H&E).

Vascular permeability assay. Vascular leakage was assessed using Evans blue dye as a marker for albumin extravasation as described previously (39). Briefly, 0.2 ml of Evans blue dye (0.5% [wt/vol] in PBS) (Sigma Aldrich) was injected intravenously into the anesthetized mice. After 2 h, the animals were euthanized and were extensively perfused with sterile PBS. Vascular permeability in the tissues was determined quantitatively; the tissues were harvested and weighed prior to dye extraction using *N*,*N*-dimethylformamide (4 ml/g of tissue [wet weight]; Sigma) at 37°C for 24 h, after which absorbance was read at 620 nm. Data are expressed as the fold increase in the optical density at 620 nm (OD_{620}) per g of tissue (wet weight) relative to the uninfected control.

Hematology. Mouse blood samples were collected in K_2-EDTA and serum tubes (Biomed Diagnostics). Levels of alanine (ALT) and aspartate (AST) transaminases and albumin in serum were quantified using a Cobas C111 chemistry analyzer (Roche).

Statistics. All statistical analysis was done with GraphPad Prism, version 5.0 (GraphPad Software, San Diego, CA). Data were analyzed by Student's *t* test. A one-tailed *P* value of <0.05 was considered significant.

Nucleotide sequence accession number. The sequence of the viral genome of D2Y98P-PP1 has been submitted to GenBank under accession number JF327392.

RESULTS

Sequence comparison between virulent strain D2Y98P-PP1 and nonvirulent strain D2MY00-22563. To ascertain the clonal origin of the D2Y98P virus strain, two consecutive rounds of plaque purification were performed. The virulence of the resulting viral suspension, named D2Y98P-PP1, was confirmed in AG129 mice and recapitulated the kinetic and clinical manifestations of the disease as described for D2Y98P (39) (data not shown). The viral genome of D2Y98P-PP1 was then fully sequenced, and a BLAST search revealed a close match with the published sequence of a DENV-2 strain isolated in Malaysia in 2000, D2MY00-22563 (GenBank accession number FN429892). Only 41 nucleotide differences between the two viruses were mapped (Table 1): 2 differences were located in the 3′ untranslated region (3′ UTR), and 39 differences resided in the open reading frame (ORF), of which 7 led to amino acid changes (MT1 to MT7, shaded in Table 1). The virulence of strain D2MY00-22563 was examined in AG129 mice and was compared to the virulence of strain D2Y98P-PP1. All mice infected with 10^6 PFU of strain D2Y98P-PP1 died by day 5 or 6 postinfection, whereas mice infected with an equal amount of strain D2MY00-22563 remained healthy throughout the experimental period (Fig. 1). These results demonstrate that despite high genome sequence identity, the D2Y98P-PP1 and D2MY00-22563 virus strains differ strikingly in their intrinsic virulence in AG129 mice, suggesting that all or some of the nucleotide differences between the two viruses account for the difference in virulence.

The F52L substitution in NS4B abolishes the virulence of the D2Y98P-PP1 virus. To identify the determinant(s) responsible for the virulence of D2Y98P-PP1, we generated an

TABLE 1. Nucleotide differences between strains D2Y98P-PP1 and D2MY00-22563[a]

No.	Nucleotide	Location[b] (aa)	Amino acid (codon) in strain:		Mutation leading to amino acid change
			D2Y98P-PP1	D2MY00-22563	
1	249	C (51)	Val (GUG)	Val (GUA)	
2	591	PrM (51)	Tyr (UAC)	Tyr (UAU)	
3	593	PrM (52)	Asn (AAU)	Ser (AGU)	MT1
4	648	PrM (70)	Ser (UCU)	Ser (UCC)	
5	725	Mem (5)	Val (GUU)	Ala (GCU)	MT2
6	880	Mem (57)	Tyr (UAU)	His (CAU)	MT3
7	1095	E (53)	Pro (CCC)	Pro (CCA)	
8	1184	E (83)	Asn (AAU)	Iso (AUU)	MT4
9	1506	E (190)	Gly (GGA)	Gly (GGC)	
10	1770	E (278)	Leu (CUA)	Leu (CUG)	
11	2377	E (481)	Leu (CUA)	Leu (UUA)	
12	2403	E (489)	Leu (UUG)	Leu (UUA)	
13	2748	NS1 (109)	Thr (ACC)	Thr (ACU)	
14	3012	NS1 (197)	Asp (GAC)	Asp (GAT)	
15	3309	NS1 (296)	Pro (CCT)	Pro (CCC)	
16	3324	NS1 (301)	Thr (ACU)	Thr (ACC)	
17	3666	NS2A (63)	Thr (ACU)	Thr (ACC)	
18	4029	NS2A (184)	Ser (UCC)	Ser (UCU)	
19	4195	NS2B (22)	Leu (UUA)	Leu (CUA)	
20	4531	NS3 (4)	Leu (UUG)	Leu (CUG)	
21	5043	NS3 (174)	Asp (GAC)	Asp (GAU)	
22	5688	NS3 (389)	Thr (ACC)	Thr (ACA)	
23	5766	NS3 (415)	Ala (GCA)	Ala (GCU)	
24	5943	NS3 (474)	Tyr (UAC)	Tyr (UAU)	
25	6009	NS3 (496)	Asp (GAU)	Asp (GAC)	
26	6684	NS4A (103)	Thr (CAU)	Thr (CAC)	
27	6729	NS4A (118)	Leu (UUG)	Leu (UUA)	
28	6775	2K (7)	Leu (UUA)	Leu (CUA)	
29	6963	NS4B (46)	Thr (ACU)	Thr (ACC)	
30	6981	NS4B (52)	Phe (UUU)	Leu (UUG)	MT5
31	7221	NS4B (132)	Glu (GAG)	Glu (GAA)	
32	7431	NS4B (202)	Ser (UCU)	Ser (UCC)	
33	7515	NS4B (230)	Leu (CUG)	Leu (CUA)	
34	8156	NS5 (196)	Ala (GCG)	Val (GUG)	MT6
35	8631	NS5 (354)	Val (GUA)	Val (GUU)	
36	8810	NS5 (414)	Asn (AAU)	Thr (ACU)	MT7
37	9078	NS5 (503)	Ser (UCC)	Ser (UCU)	
38	9297	NS5 (576)	Lys (AAA)	Lys (AAG)	
39	10179	NS5 (870)	Val (GUU)	Val (GUC)	
40	10343	3′ UTR	U	C	
41	10403	3′ UTR	G	U	

[a] Obtained from sequence alignment. The seven nucleotide differences that lead to amino acid changes are shaded and designated MT1 to MT7.
[b] C, capsid; PrM, premembrane; E, envelope; Mem, membrane.

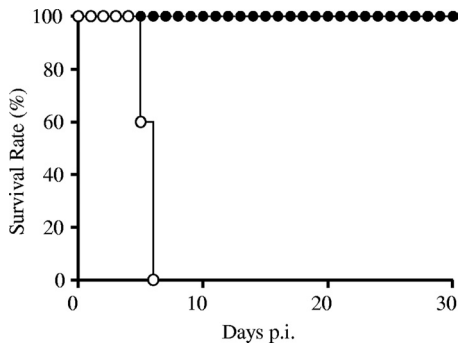

FIG. 1. Survival rates of mice infected with the D2Y98P-PP1 or D2MY00-22563 virus strain. AG129 mice (10 animals per group) were administered approximately 10^6 PFU of virus strain D2Y98P-PP1 (open circles) or D2MY00-22563 (solid circles) i.p. Survival was monitored daily, and mice that were moribund, as evidenced by severe diarrhea, lethargy, and dramatic body weight loss, were euthanized. The experiment was performed twice independently.

infectious cDNA clone of the D2Y98P-PP1 virus. The infectious clone (IC)-derived virus, named D2Y98P-PP1-IC, exhibited a plaque morphology similar to that of the parental D2Y98P-PP1 virus (data not shown). Genome-length sequencing showed no mutations between the parental D2Y98P-PP1 and D2Y98P-PP1-IC viruses. Importantly, the D2Y98P-PP1-IC virus showed morbidity and mortality comparable to those of the parental D2Y98P-PP1 virus in AG129 mice (compare Fig. 2C with Fig. 1), demonstrating that the infectious clone-derived virus recapitulates the virulence of the parental virus.

Using D2Y98P-PP1-IC, seven mutant viruses (MT1 to MT7 [Table 1]) were generated. Each mutant contained a single amino acid mutation that corresponded to the amino acid found at the same position in the nonvirulent D2MY00-22563 virus strain (Fig. 2A). Plaque assays showed that the plaques obtained with MT5 were slightly smaller than those obtained with D2Y98P-PP1-IC and the other mutants and

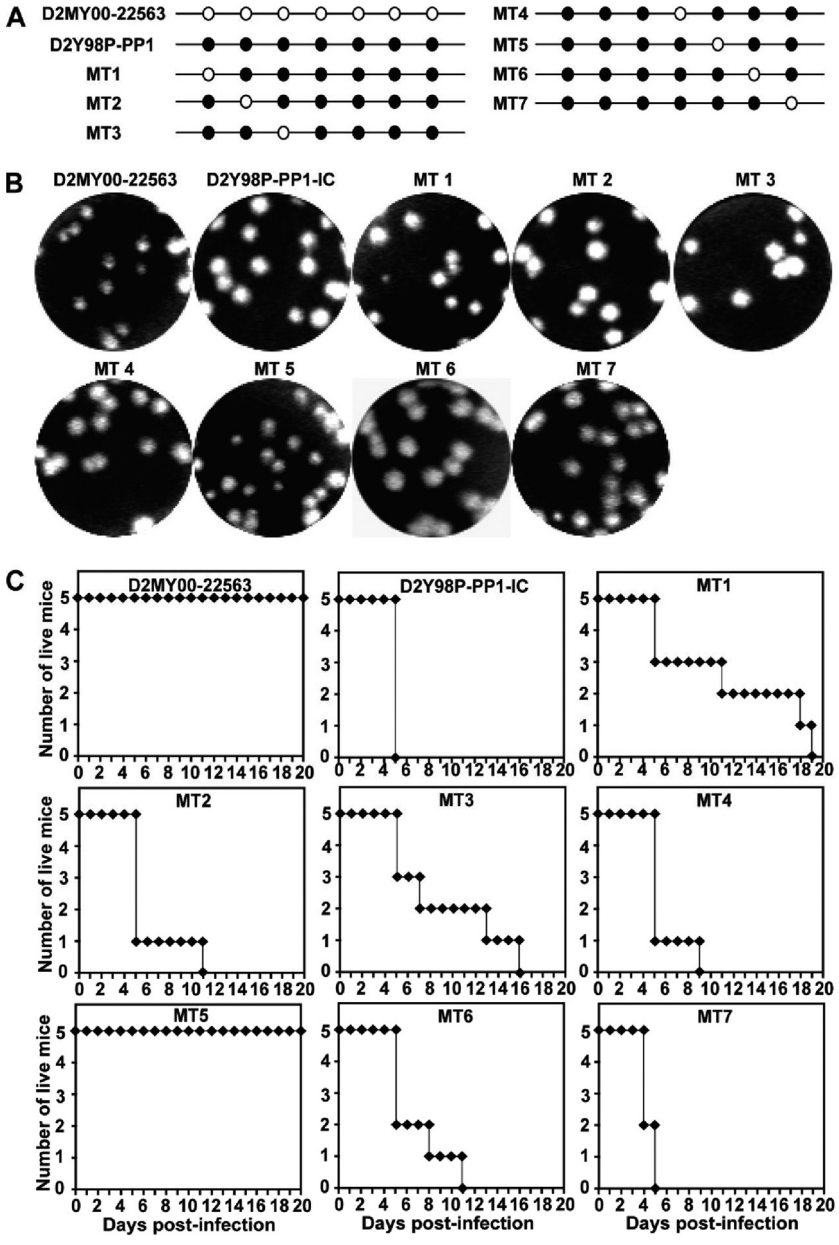

D

	D2MY00-22563	D2Y98P-PP1	MT1	MT2	MT3	MT4	MT5	MT6	MT7
Morbidity (%)	0	100	100	100	100	100	0	100	100
Mortality (%)	0	100	100	100	100	100	0	100	100
Average survival time (days)	-	5	11.6	6.02	9.02	5.8	-	6.8	4.5

FIG. 2. Plaque morphology and virulence in mice of virus mutant strains harboring a single amino acid substitution in the D2Y98P-PP1 genome. (A) Graphical representation of the seven mutant viruses (MT1 to MT7) derived from D2Y98P-PP1-IC. Each mutant virus contains a single amino acid change to one of the seven amino acids found in D2MY00-22563. (B) Plaque morphologies of the D2MY00-22563, D2Y98P-PP1-IC, and MT1 to MT7 viruses in BHK-21 cells. (C) Survival rates of AG129 mice infected with the indicated viruses. AG129 mice were inoculated i.p. with approximately 4×10^6 PFU of the indicated viruses (5 mice per group). (D) Summary of morbidity and mortality rates, and average survival times, from the results shown in panel C. Average survival times were calculated only for mice that died.

were comparable in size to the plaques obtained with D2MY00-22563 (Fig. 2B).

The virulence of mutant viruses MT1 to MT7 was then examined in AG129 mice and was compared to the virulence of the D2Y98P-PP1-IC and D2MY00-22563 viruses. Upon i.p. inoculation of 4.6×10^6 PFU of MT5, none of the infected mice showed any signs of disease; no death was observed throughout the course of the experiment (Fig. 2C). As ex-

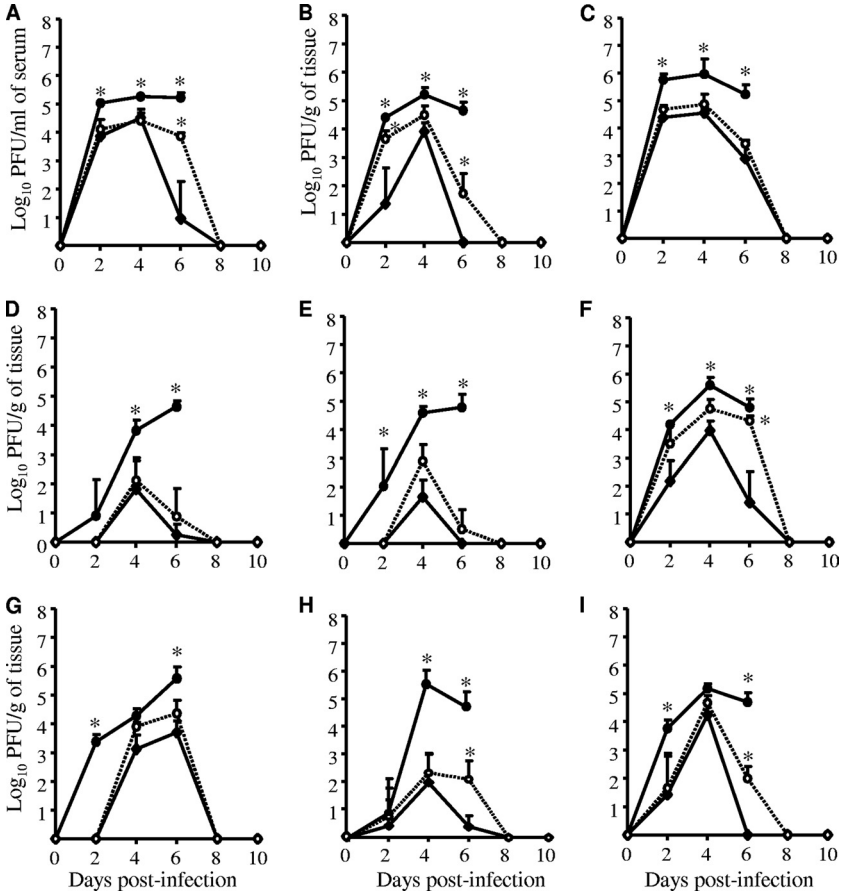

FIG. 3. Virus loads in mice infected with strain D2Y98P-PP1, D2MY00-22563, or MT5. Mice were infected i.p. with approximately 10^6 PFU of strain D2Y98P-PP1 (solid circles), D2MY00-22563 (solid diamonds), or MT5 (open circles connected by dotted lines), and the viral loads in the blood (A), liver (B), spleen (C), brain (D), spinal cord (E), kidney (F), skin (G), intestines (H), and lungs (I) were monitored over time as indicated and were quantified by plaque assays. Five mice per time point were assessed individually. Asterisks indicate results significantly different (*, $P < 0.05$) from those for the D2MY00-22563-infected group.

pected, mice infected with an equal amount of the D2MY00-22563 virus showed no morbidity or mortality. In contrast, mice infected with mutant MT1, -2, -3, -4, -6, or -7, or with the D2Y98P-PP1-IC virus, displayed signs of disease by day 4 postinfection; at least two mice died by day 5; and all mice died by day 19 (Fig. 2C). Figure 2D summarizes the morbidity and mortality rates and the average survival times of infected mice. The average survival time for mice infected with mutant MT1, -2, -3, -4, or -6 was significantly higher than that of the D2Y98P-PP1-IC-infected group, suggesting that the amino acids replaced in these mutants may also contribute to overall virus virulence. However, MT5 was the only mutant that led to 100% survival, supporting the notion that the amino acid replaced in this mutant plays a critical role in the virulence of the D2Y98P-PP1 virus.

Since MT5 displayed the most drastic phenotypic change based on the survival rate, we decided to further characterize the effect of the amino acid substitution in this mutant. MT5 contains an F52L substitution in NS4B protein (Table 1). The viral loads in the blood and in various organs were monitored over the course of infection in MT5-infected AG129 mice and were compared with the viral loads in D2MY00-22563- and D2Y98P-PP1-infected animals. The results indicate that the replication kinetics of MT5 were comparable to those of the D2MY00-22563 virus, with a peak of viral production at day 4 postinfection, followed by progressive clearance within 8 days (Fig. 3). In contrast, D2Y98P-PP1 replication reached a peak at days 4 to 6 postinfection, which coincided with the animals' death (Fig. 3). Remarkably, the numbers of infectious viral particles harvested from the blood and various organs of D2Y98P-PP1-infected mice were generally significantly higher than those for D2MY00-22563- and MT5-infected animals, suggesting that the D2Y98P-PP1 virus replicated more effectively in mice than the other two virus strains.

Furthermore, vascular leakage, a hallmark of severe dengue in humans and one of the clinical manifestations observed in D2Y98P-infected mice (39), was measured by an Evans blue assay in MT5-infected mice and was compared to that with its parental counterpart D2Y98P-PP1 and strain D2MY00-22563. Whereas substantial leakage was found in the livers, kidneys, spleens, and intestines of D2Y98P-PP1-infected animals, as evidenced by >2-fold changes in absorbance readings from those for noninfected controls, no increase in vascular permeability was detected in the D2MY00-22563- and MT5-infected groups (<2-fold changes) (Fig. 4A to C). Increased vascular permeability was confirmed by a drop in the serum albumin

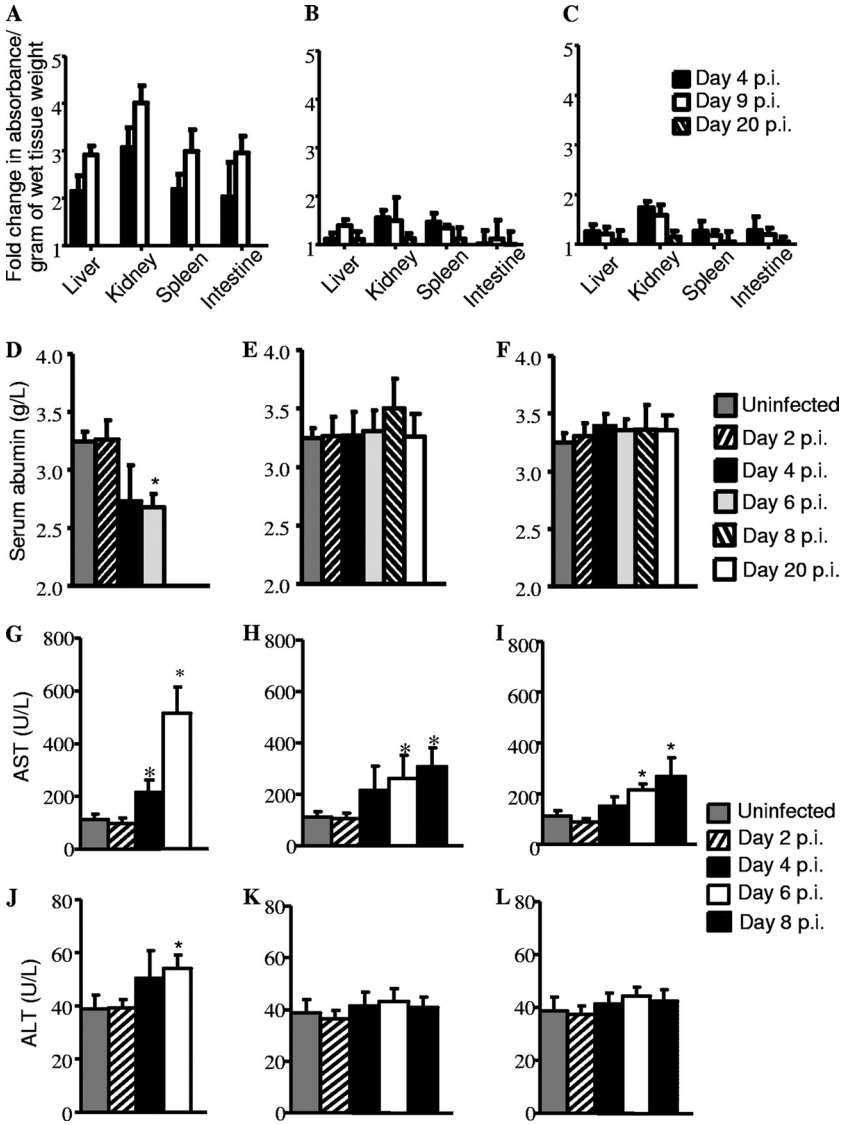

FIG. 4. Vascular permeability and blood parameters in mice infected with strain D2Y98P-PP1, D2MY00-2263, or MT5. Mice were infected i.p. with approximately 10^6 PFU of strain D2Y98P-PP1 (A, D, G, and J), D2MY00-22563 (B, E, H, and K), or MT5 (C, F, I, and L), and vascular permeability (A to C) and serum albumin (D to F), AST (G to I), and ALT (J to L) concentrations were monitored over time as indicated. Vascular permeability was assessed by an Evans blue extravasation assay as described in Materials and Methods. Five mice per time point were individually processed. Asterisks indicate results significantly different (*, $P < 0.05$) from those for the uninfected group.

concentration in D2Y98P-PP1-infected mice but not in the other groups (Fig. 4D to F). Liver dysfunction, reflected by increased levels of alanine (ALT) and aspartate (AST) transaminases in serum, is also a clinical feature in DEN patients (8) and in D2Y98P-infected mice (39). Increased AST and ALT levels were detected in D2Y98P-PP1-infected mice, whereas a milder increase (AST) or no increase (ALT) was detected in the D2MY00-22563- and MT5-infected groups (Fig. 4G to L). Finally, histology analysis of livers, spleens, and intestines from the infected animals revealed no major histopathological signs in D2MY00-22563- and MT5-infected mice, whereas D2Y98P-PP1-infected animals displayed disorganization of the spleen architecture, hepatic necrosis characterized by pyknotic nuclei and cytoplasmic vacuolation of hepatocytes, and severe damage of the intestinal tissue, as reported previously (39) (Fig. 5).

Taken together, these results demonstrate that the Phe-to-Leu alteration at amino acid position 52 of NS4B completely abolished the virulence of the D2Y98P-PP1-IC virus; some other mutations (such as MT1 and MT3) also reduced virulence, as evidenced by delayed death of the animals, but to a much lesser extent. These results allowed us to conclude that Phe at position 52 of NS4B is critical for the virulence of the D2Y98P-PP1 virus.

The NS4B(L52F) substitution confers virulence on a nonvirulent DENV-2 strain. To further demonstrate that a Phe residue at position 52 of NS4B is a key virulence determinant, we asked whether this NS4B mutation could convert the non-

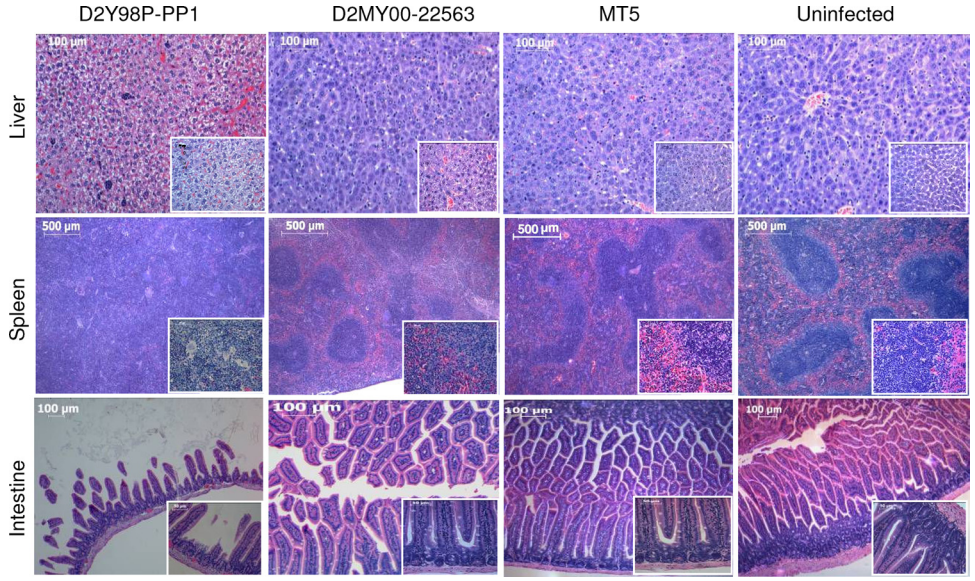

FIG. 5. Liver, spleen, and intestine histology of mice infected with strain D2Y98P-PP1, D2MY00-22563, or MT5. Mice were either left uninfected or infected i.p. with approximately 10^6 PFU of strain D2Y98P-PP1, D2MY00-22563, or MT5, and the animals were euthanized at the moribund stage (day 6 p.i. for D2Y98P-PP1-infected mice) or at day 9 p.i. (for uninfected, D2MY00-22563-infected, and MT5-infected animals). The liver, spleen, and intestines were harvested and processed for H&E staining. Observations were made at magnifications of ×200 (liver), ×100 (intestine), and ×50 (spleen), or at higher magnifications (shown at the bottom right of each panel): ×400 (liver), ×200 (intestine), and ×100 (spleen). Five mice per group were processed and analyzed.

virulent DENV-2 strain TSV01 into a virulent virus in AG129 mice. The rationale for choosing strain TSV01 was as follows. (i) There are only seven amino acid differences between strains D2Y98P-PP1 and TSV01 (Fig. 6A). Importantly, TSV01 NS4B harbors Leu at amino acid position 52, which is identical to the residue in the nonvirulent strain D2MY00-22563 described above. (ii) An infectious cDNA clone and a replicon system for DENV-2 strain TSV01 are available in our laboratory, allowing mutagenesis approaches.

An NS4B(L52F) substitution was thus introduced into the cDNA infectious clone of TSV01. Interestingly, the TSV01 NS4B(L52F) virus gave rise to plaques in BHK cells that were larger than those of wild-type (WT) TSV01 but smaller than those of the D2Y98P-PP1 virus (Fig. 6B). AG129 mice inoculated with 5×10^5 PFU of the TSV01 NS4B(L52F) virus showed 80% mortality (Fig. 6C) and 100% morbidity, with clinical manifestations similar to those developed by animals infected with a similar dose of the D2Y98P-PP1 virus, including ruffled fur and a hunched back, followed by severe diarrhea at the moribund stage (Fig. 6D). In contrast, mice infected with 5×10^5 PFU WT TSV01 did not die and remained healthy throughout the course of the experiment and up to 20 days postinfection (Fig. 6C and D). In addition, the viremia titers in TSV01 NS4B(L52F)-infected mice were monitored over time and were found to be significantly higher than those in the WT TSV01-infected group (Fig. 6E). Interestingly, despite viral clearance from the bloodstream by day 10 p.i., the TSV01 NS4B(L52F)-infected animals that were still alive by then displayed disease manifestations and died by day 12 p.i., findings similar to previous observations made with a low infectious dose of D2Y98P (39).

Taken together, these results demonstrate that NS4B(L52F) substitution is sufficient to convert the nonvirulent DENV-2 strain TSV01 into a virulent virus in mice.

NS4B(L52F) substitution enhances virus production in a type I IFN-independent manner. Since the viral loads detected in MT5-infected mice were significantly lower than those detected in the D2Y98P-PP1-infected group (Fig. 3), we reasoned that the F52L substitution in NS4B may result in lower viral replication efficacy. Consistently, the level of viral production by MT5 (and D2MY00-22563) in Vero and BHK-21 mammalian cells was significantly lower than that by D2Y98P-PP1 (Fig. 7A and B). In contrast, the level of viral production by MT5 in C6/36 cells was not significantly different from that of its parental counterpart (Fig. 7C). A comparable trend was observed when virus titers were determined in the culture supernatants (Fig. 7D to F), suggesting that the main step of the infection cycle affected by the NS4B(F52L) substitution occurs during intracellular viral replication, and not at the later stages of the cycle, i.e., particle release efficacy and/or viral spread.

Similarly, the level of virus production by TSV01 was found to be lower than that by TSV01 NS4B(L52F) in BHK-21, Vero, and A549 mammalian cells (see Fig. S2 in the supplemental material), whereas these viruses replicated with comparable efficiency in C6/36 mosquito cells (see Fig. S2).

DENV NS4B protein has been shown to antagonize the innate immune response, thereby allowing greater virus production (30). We thus hypothesized that the NS4B(L52F) substitution could enhance the ability of NS4B to inhibit the IFN response, leading to enhanced viral replication in mammalian cells. To test this hypothesis, the IFN-mediated phosphorylation of STAT1 was monitored in BHK-21 cells expressing HA-tagged NS4B(L52) or NS4B(F52) protein. At 24 h post-

A

Location	TSV01	D2Y98P-PP1
Membrane (aa 71)	Thr (ACU)	Ala (GCU)
NS2B (aa 112)	Ala (GCG)	Val (GUG)
NS3 (aa 160)	Ala (GCA)	Thr (ACA)
NS4B (aa 19)	Ala (GCA)	Thr (ACA)
NS4B (aa 52)	Leu (UUG)	Phe (UUU)
NS5 (aa 414)	Thr (ACU)	Asn (AAU)
NS5 (aa 570)	Lys (AAA)	Arg (AGA)

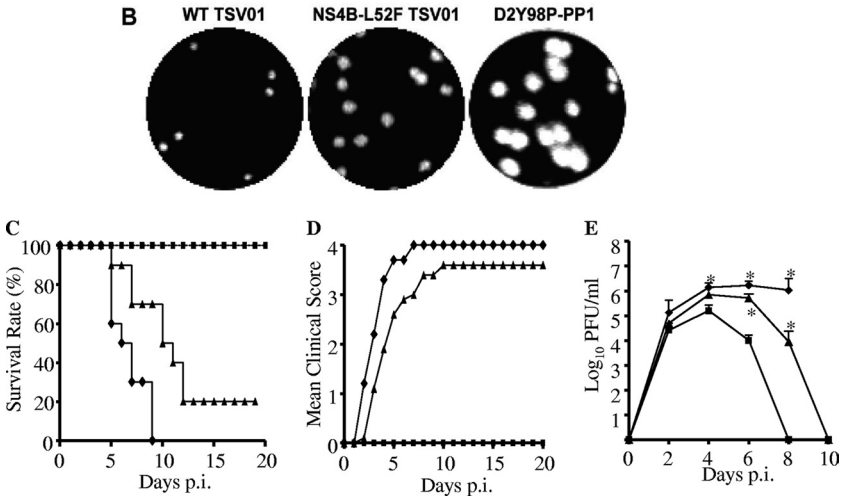

FIG. 6. Plaque morphology and virulence in mice infected with the WT TSV01 or TSV01 NS4B(L52F) virus strain. (A) Differences in amino acid sequence between the TSV01 and D2Y98P-PP1 strains. (B) Plaque morphologies of the WT TSV01, TSV01 NS4B(L52F), and D2Y98P-PP1 viruses in BHK-21 cells. (C to E) AG129 mice were infected i.p. with 5×10^5 PFU of the WT TSV01 (squares), TSV01 NS4B(L52F) (triangles), or D2Y98P-PP1 (diamonds) virus. The survival rate (C) (10 mice per group) and clinical manifestations (D) (10 mice per group) were monitored and scored as follows: 0, healthy; 1, ruffled fur; 2, hunched back; 3, diarrhea; 4, moribund stage. Viremia was measured at the indicated time points (E) (5 mice per group per time point). Asterisks indicate results significantly different (*, $P < 0.05$) from those for the WT TSV01-infected group. Each experiment was performed at least twice independently.

transfection (p.t.), the cells were treated with IFN-α (500 U/ml), and phosphorylated STAT1 levels were assessed by immunofluorescence. Whereas cells transfected with the empty vector (no NS4B protein expression) exhibited strong nuclear staining of phosphorylated STAT1, reduced levels of phosphorylated STAT1 were observed both for cells expressing HA-NS4B(L52) and for those expressing HA-NS4B(F52) protein (Fig. 8A). These observations thus confirm that NS4B mediates the suppression of the IFN response, as reported previously (30), and they indicate that this suppressive effect is independent of whether a Leu or a Phe residue is present at position 52 in NS4B protein.

To further confirm our observations, a second assay was performed using a firefly luciferase reporter system cloned downstream of an interferon-stimulated response element (ISRE). 293T cells were cotransfected with a pISRE-Luc plasmid and a plasmid expressing either HA-NS4B(L52) or HA-NS4B(F52) protein. In addition, plasmid phRL-TK, expressing *Renilla* luciferase, was cotransfected to assess transfection efficiency. At 24 h posttransfection, the cells were treated with IFN-β (1,000 U/ml) for another 24 h, after which they were assayed for firefly luciferase activities. HA-NS4B(L52)- and HA-NS4B(F52)-expressing cells displayed comparable suppression of the IFN-β-mediated induction of firefly luciferase expression, by 55% and 48%, respectively (Fig. 8B). Western blotting indicated that NS4B(L52)-HA and NS4B(L52)-HA were expressed at equivalent levels in the transfected cells (Fig. 8C).

Taken together, these results indicate that the L52F substitution does not affect the ability of NS4B protein to interfere with the host IFN pathway, thereby ruling out the possibility that the enhanced viral replication of D2Y98P-PP1 and TSV01 NS4B(L52F) observed *in vivo* and *ex vivo* is due to a greater ability to suppress the host IFN response.

NS4B(L52F) substitution enhances viral RNA synthesis in mammalian cells. To better understand the mechanisms involved in the greater replication ability of the D2Y98P-PP1 virus, viral RNA synthesis was monitored over time in Vero, BHK-21, and C6/36 cells by real-time PCR and was compared to that of strains MT5 and D2MY00-22563. The results indicate that the level of RNA synthesis of the D2Y98P-PP1 virus upon infection of mammalian Vero and BHK-21 cells was much higher than that of the MT5 and D2MY00-22563 viruses (Fig. 9A and B). However, no significant difference in RNA synthesis was found between the three viruses in C6/36 mosquito cells (Fig. 9C).

To further demonstrate that the F52L substitution in NS4B accounts for the differential viral RNA synthesis efficacy, a luciferase reporter assay was performed using WT TSV01 and TSV01 NS4B(L52F) replicons containing a luciferase gene

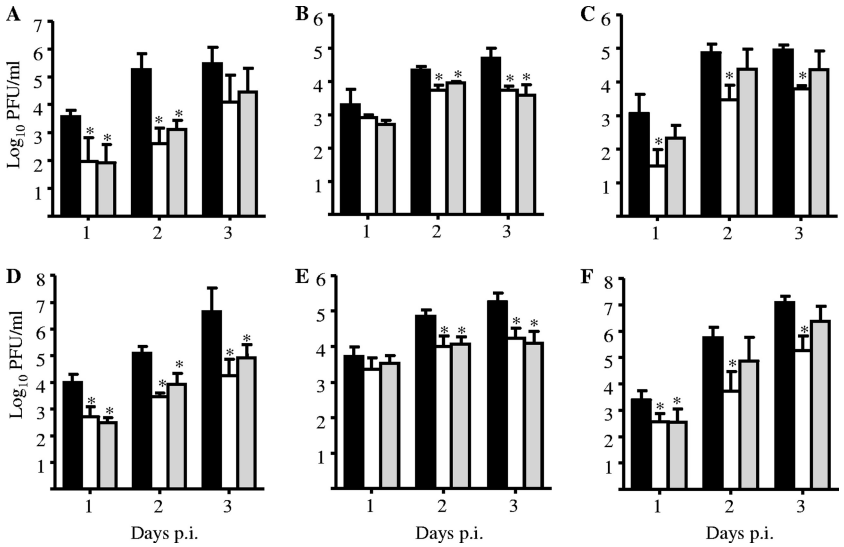

FIG. 7. Viral production in mammalian and mosquito cell lines. Vero (A and D), BHK-21 (B and E), and C6/36 (C and F) cells were infected with strain D2Y98P-PP1 (filled bars), D2MY00-22563 (open bars), or MT5 (shaded bars) at an MOI of 0.005 (Vero cells), 0.006 (BHK-21 cells), or 0.0025 (C6/36 cells). At the indicated time points postinfection, the supernatants were harvested (D to F), the infected-cell monolayers were washed and lysed (A to C), and the numbers of viral infectious particles in both the supernatants and the cell lysates were assessed by plaque assays. Results are expressed as averages ± SDs for triplicate experiments. Asterisks indicate significant differences ($P < 0.05$) from the results for the D2Y98P-PP1-infected group. The experiment was performed twice independently.

fused in frame with the viral ORF (33). Equal amounts of WT and mutant replicon RNAs were electroporated into mammalian (BHK-21, Vero, A549) and mosquito (C6/36) cells (data not shown). The cells were assayed for luciferase activities at various time points posttransfection. Upon transfection into mammalian cells, the WT and NS4B(L52F) mutant replicons produced similar levels of luciferase signals at 2 to 6 h posttransfection, indicating that the NS4B(L52F) substitution does not affect viral translation (Fig. 10A to C) (26). In contrast, at 21 h to 45 h posttransfection, the mutant replicon generated higher luciferase signals than the WT replicon (Fig. 10A to C), whereas the two replicons generated comparable luciferase signals in mosquito cells throughout the course of the experiment (Fig. 10D). These results are thus consistent with the real-time PCR data obtained with the MT5 and D2Y98P-PP1 viruses (Fig. 9) and demonstrate that the L52F substitution in

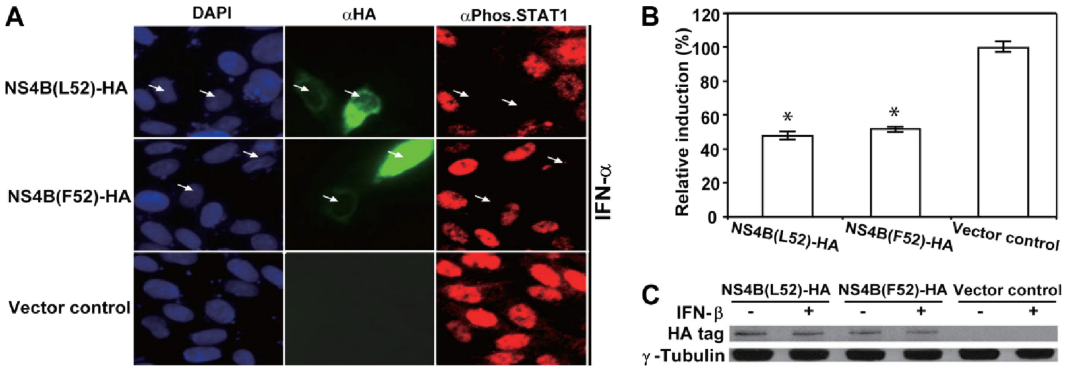

FIG. 8. Inhibition of IFN-mediated STAT1 phosphorylation by NS4B(L52) and NS4B(F52) proteins. (A) BHK-21 cells were transfected with plasmids expressing NS4B(L52)-HA, NS4B(F52)-HA, or an empty vector (control) as indicated. At 24 h posttransfection, the cells were treated with IFN-α (500 U/ml), followed by immunofluorescence staining. The NS4B(L52)-HA and NS4B(F52)-HA proteins (green) and phosphorylated STAT1 (Phos.STAT1) (red) were detected with antibodies (α). Arrows indicate cells with no or low levels of nuclear staining of phosphorylated STAT1 and high expression of NS4B(L52) or NS4B(F52). (B) 293T cells were cotransfected with a pISRE-Luc (firefly luciferase) plasmid and a plasmid expressing the NS4B(L52)-HA or NS4B(F52)-HA protein. An empty vector was included as a control. At 24 h posttransfection, the cells were either left untreated or treated with human IFN-β (1,000 U/ml). After 24 h of incubation, the cells were assayed for firefly luciferase and *Renilla* luciferase activities. Average relative induction values (compared with values for empty-plasmid-transfected cells) from at least three independent experiments are shown. Error bars represent SDs (n, ≥3). Asterisks indicate results significantly different (*, $P < 0.05$) from those for the empty-vector-transfected group. (C) Western blotting for NS4B expression. At the time of the luciferase assay (24 h after IFN-β treatment), cell lysates were analyzed for NS4B expression using an antibody against the HA tag. Tubulin was used to normalize the loading of cell lysates. Lysates from cells transfected with different plasmids [a plasmid expressing NS4B(L52)-HA, a plasmid expressing NS4B(F52)-HA, and an empty-vector plasmid], as well as IFN-β treatment, are indicated.

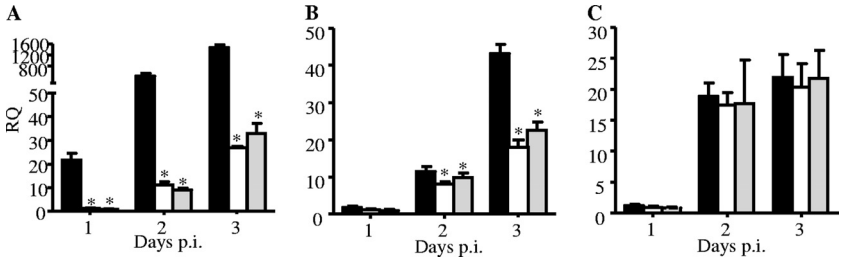

FIG. 9. Viral RNA synthesis in mammalian and mosquito cells infected with strain D2Y98P-PP1, MT5, or D2MY00-22563. Vero (A), BHK-21 (B), and C6/36 (C) cells were infected with strain D2Y98P-PP1 (filled bars), D2MY00-22563 (open bars), or MT5 (shaded bars) at an MOI of 0.005 (Vero cells), 0.006 (BHK-21 cells), or 0.0025 (C6/36 cells). At the indicated time points postinfection, the cells were harvested, and viral RNA was extracted. Real-time PCR analysis was performed as described in Materials and Methods. Results are expressed as the relative quantity (RQ) of the C_T value compared to that obtained with D2MY00-22563 at day 1 p.i. Asterisks indicate significant differences (*, $P < 0.05$) from the results for the D2Y98P-PP1-infected group. The experiment was performed twice independently.

NS4B protein enhances viral RNA synthesis in a host species-dependent manner.

DISCUSSION

It is generally believed that DEN pathogenesis results from the interplay of multiple factors contributed by both the host and the virus. The hypothesis that viral determinants play a role in DENV intrinsic virulence was first proposed by Barnes and Rosen based on the 1972 DENV-2 epidemic in Niue Island in the South Pacific region, which was characterized by a high incidence of hemorrhagic manifestations and deaths in a region where no sign of DEN activity had been evident over a 25-year period prior to the epidemic (2, 36). Among the many field studies that reported an association of the viral genotype with DEN epidemics and severity, the study conducted in Puerto Rico was probably the most convincing and compelling: first introduced in Puerto Rico in 1982, DENV-2 did not cause an outbreak until 1994, when the virus was associated with a clade change (3). Subsequently, similar observations were made in Sri Lanka (27), Singapore (21), and Vietnam (44). Further evidence based on molecular epidemiological studies in conjunction with clinical data supported the notion that the risk of DHF due to DENV strains of the Asian genotype is greater than that for the American DENV strains, which lead to milder disease (32, 45).

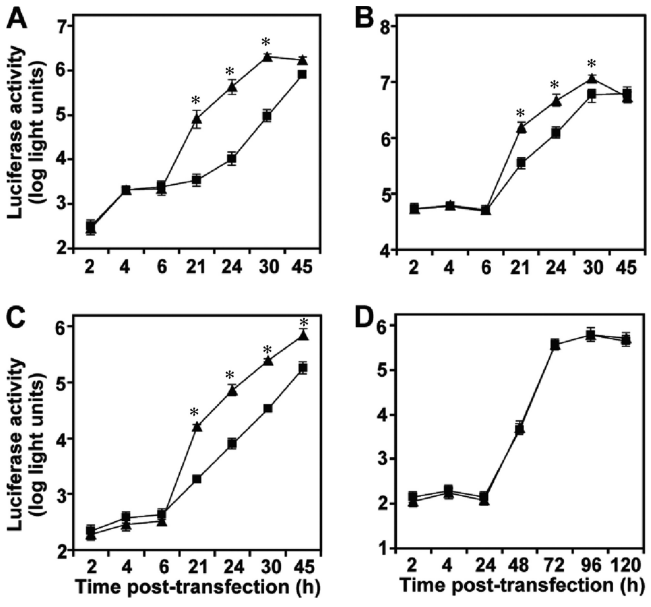

FIG. 10. Effects of NS4B(L52F) mutation on viral translation and RNA synthesis as determined by a transient replicon assay. Vero (A), BHK-21 (B), A549 (C), and C6/36 (D) cells were electroporated with equal amounts of WT (■) or NS4B(L52F) (▲) TSV01 *Renilla* luciferase replicon RNAs (10 mg) and were assayed for luciferase activities at the indicated time points. Results are expressed as means ± SDs of triplicates. Asterisks indicate significant differences (*, $P < 0.05$) from the results for the WT replicon-electroporated group. The experiment was performed twice independently.

We report here the identification of a novel critical virulence determinant in DENV. We recently characterized a non-mouse-adapted DENV-2 strain (D2Y98P) that is highly virulent in AG129 mice, leading to the animals' death with severe organ damage or dysfunction and increased vascular permeability (39). The original D2Y98P virus was isolated in 1998 from a DENV-infected patient in Singapore. Unfortunately, the clinical information and disease outcome of the patient were not documented. In this work, we show that a Phe-to-Leu alteration at position 52 in the NS4B protein of the plaque-purified D2Y98P-PP1 strain led to reduced viral RNA synthesis in mammalian cells, which resulted in smaller plaques *in vitro* and lower viral loads in infected mice. Importantly, these features correlated with the abolition of virulence/pathogenesis in mice, as evidenced by the lack of lethality, the absence of clinical and histological signs of disease, and intact vascular permeability. These observations thus strongly supported the idea that a Phe residue at position 52 in NS4B plays a critical role in the virulence of strain D2Y98P-PP1. However, since the amino acids substituted in mutants MT1 to MT4 and MT6 led to delayed death of the infected animals (Fig. 2C), these residues may also play a role in the overall virulence of the D2Y98P-PP1 virus.

Furthermore, we demonstrated that replacing Leu with Phe at position 52 of NS4B in the nonvirulent strain TSV01 was sufficient to confer virulence on this virus, as evidenced by an 80% death rate. The amino acid substitution in TSV01 NS4B resulted in greater viral RNA synthesis in mammalian cells *ex vivo* and increased viremia *in vivo*. Thus, our work identifies a novel key viral virulence determinant and supports a correlation between replication efficiency, viral loads, and virulence/

pathogenesis in mice. Consistently, a number of studies have suggested that higher viremia is a feature of severe DEN in humans (23, 40, 43), and such a correlation constitutes the rationale for the development of drugs and monoclonal antibodies that target DENV particles. However, we cannot totally rule out the possibility that the DENV strains compared may have different virus particle-to-PFU ratios and that the noninfectious particles may contribute to the virulence outcome of each virus. But the chances that variance in noninfectious particles among the different viruses contributes to virulence are low, in particular when one considers that the DENV strains that were compared differ only by a single amino acid in NS4B in their whole genomes.

Specific mutations altering viral replication efficacy that resulted in virulence attenuation have been identified previously mainly in the 3′ and 5′ noncoding regions of the DENV genome and have driven the selection of live attenuated DENV vaccine candidates (6, 20, 34). It was proposed that mutations in these untranslated regions result in alterations of the secondary structure and folding of the RNA molecule that would impair its stability and/or affect replication efficacy. In addition, mutations in the NS3, NS4B, and NS5 proteins have been reported to affect viral replication efficacy; however, these mutations did not necessarily correlate with a change in virulence in animal models (5).

We demonstrated here that a Phe-to-Leu alteration at position 52 in NS4B protein significantly reduced the efficacy of viral RNA synthesis in mammalian cells. NS4B is a transmembrane protein that participates in the formation of the viral replication complex (24) and, as such, plays a critical role in viral RNA synthesis. DENV-2 NS4B has been shown to interact physically with NS3; the NS3–NS4B interaction dissociated NS3 from single-strand RNA and enhanced NS3 helicase activity (42). Whereas NS4B proteins display marked amino acid sequence heterogeneity, their hydrophobicity profiles are remarkably conserved among DENVs and flaviviruses in general (22). Study of NS4B topology predicts five transmembrane motifs (TM1 to TM5). However, a biochemical approach indicated that TM1 and TM2 are not membrane associated; instead, they are located in the lumen of the endoplasmic reticulum (ER) (28). Thus, on the basis of this topology model, amino acid 52 (located in TM1) is unlikely to interact physically with NS3, which is located on the cytoplasmic face of the ER, after the viral polyprotein has been fully processed by viral and host proteases. However, it is possible that transient interactions between NS3 and NS4B TM1 could occur before the polyprotein is processed; such transient interactions may modulate DENV replication. Furthermore, interestingly, we found that the NS4B(L52F) substitution-mediated enhancement of viral replication is host species dependent: increased viral RNA synthesis was found in various mammalian cells, whereas unchanged RNA synthesis was observed in mosquito cells. A previous study reported that an NS4B P101L substitution in DENV-4 increased viral replication in mammalian cells but decreased viral replication in C6/36 cells (14). Amino acid 101 is located in the TM3 domain of NS4B, which, like the TM1 domain, protrudes into the ER lumen. Collectively, these observations suggest that the NS4B amino acids at position 52 in TM1 and position 101 in TM3 play a critical role in the efficacy of viral RNA synthesis, possibly through an interaction(s) with a yet unknown mammalian host factor. In addition, we have shown that the nature of the amino acid at position 52 in NS4B does not seem to affect the ability of the protein to impair the host IFN response, supporting the notion that NS4B protein is involved in various viral functions with independent functional domains.

It is not currently known whether the presence of a Phe residue at position 52 in D2Y98P-PP1 NS4B originates from the clinical isolate or from an event that occurred during *in vitro* culture. The D2Y98P virus was exclusively amplified in C6/36 mosquito cells. Considering that NS4B(L52F) does not result in enhanced viral RNA synthesis in these cells, this mutation has not conferred any selective advantage on the variant. This observation would thus support the possibility of the presence of NS4B Phe52 in the original clinical isolate. However, analysis of the NS4B protein sequences from more than 2,000 DENV strains revealed that none harbors a Phe residue at position 52 (data not shown). Either a Leu or a Met residue was found at this position, suggesting that Phe at position 52 in DENV NS4B protein either does not exist naturally or is extremely unusual.

In conclusion, our work identifies a novel critical virulence determinant in DENV that modulates the efficacy of viral RNA synthesis and is associated with virulence/pathogenesis in the mouse model. While our study and others, by the identification of various molecular viral determinants, have provided proof of principle that the viral genome sequence contributes to DENV virulence *in vivo* in mouse models, the relative contributions of these determinants to virulence in humans remain a matter of debate. Nevertheless, the identification of DENV mutant strains with altered replication and/or host binding capacities has been the basis for the selection and design of live attenuated DENV vaccine candidates currently undergoing clinical trial in humans. Thus, in addition to providing further insights into the role of NS4B during viral replication, our findings may be of interest for the rational design of the next generation of live attenuated DENV vaccine candidates.

ACKNOWLEDGMENTS

We are grateful to Shamala Devi (Department of Medical Microbiology, University of Malaya, Kuala Lumpur, Malaysia) for sharing the D2MY00-22563 strain. We thank our colleagues at Novartis Institute for Tropical Diseases for helpful discussions and technical support during the course of this study.

This work was partially funded by the National Medical Research Council in Singapore (TCR flagship program "STOP Dengue," allocated to S.A.).

REFERENCES

1. **Ashour, J., M. Laurent-Rolle, P.-Y. Shi, and A. Garcia-Sastre.** 2009. NS5 of dengue virus mediates STAT2 binding and degradation. J. Virol. **83:**5408–5418.
2. **Barnes, W. J., and L. Rosen.** 1974. Fatal hemorrhagic disease and shock associated with primary dengue infection on a Pacific island. Am. J. Trop. Med. Hyg. **23:**495–506.
3. **Bennett, S. N., et al.** 2003. Selection-driven evolution of emergent dengue virus. Mol. Biol. Evol. **20:**1650–1658.
4. **Best, S. M., et al.** 2005. Inhibition of interferon-stimulated JAK-STAT signaling by a tick-borne flavivirus and identification of NS5 as an interferon antagonist. J. Virol. **79:**12828–12839.
5. **Blaney, J. E. Jr., et al.** 2003. Mutations which enhance the replication of dengue virus type 4 and an antigenic chimeric dengue virus type 2/4 vaccine candidate in Vero cells. Vaccine **21:**4317–4327.
6. **Blaney, J. E. Jr., et al.** 2008. Dengue virus type 3 vaccine candidates generated by introduction of deletions in the 3′ untranslated region (3′-UTR) or

by exchange of the DENV-3 3′-UTR with that of DENV-4. Vaccine **26:**817–828.
7. **Bray, M., R. Men, I. Tokimatsu, and C. J. Lai.** 1998. Genetic determinants responsible for acquisition of dengue type 2 virus mouse neurovirulence. J. Virol. **72:**1647–1651.
8. **Burke, D. S., A. Nisalak, D. E. Johnson, and R. M. Scott.** 1988. A prospective study of dengue infections in Bangkok. Am. J. Trop. Med. Hyg. **38:**172–180.
9. **Durbin, A. P., and S. S. Whitehead.** 2010. Dengue vaccine candidates in development. Curr. Top. Microbiol. Immunol. **338:**129–143.
10. **Engel, A. R., et al.** 2010. The neurovirulence and neuroinvasiveness of chimeric tick-borne encephalitis/dengue virus can be attenuated by introducing defined mutations into the envelope and NS5 protein genes and the 3′ noncoding region of the genome. Virology **405:**243–252.
11. **Gualano, R. C., M. J. Pryor, M. R. Cauchi, P. J. Wright, and A. D. Davidson.** 1998. Identification of a major determinant of mouse neurovirulence of dengue virus type 2 using stably cloned genomic-length cDNA. J. Gen. Virol. **79:**437–446.
12. **Guo, J., J. Hayashi, and C. Seeger.** 2005. West Nile virus inhibits the signal transduction pathway of alpha interferon. J. Virol. **79:**1343–1350.
13. **Halstead, S. B.** 2007. Dengue. Lancet **370:**1644–1652.
14. **Hanley, K., et al.** 2003. A trade-off in replication in mosquito versus mammalian systems conferred by a point mutation in the NS4B protein of dengue virus type 4. Virology **312:**222–232.
15. **Helt, A. M., and E. Harris.** 2005. S-phase-dependent enhancement of dengue virus 2 replication in mosquito cells, but not in human cells. J. Virol. **79:** 13218–13230.
16. **Julander, J. G., S. T. Perry, and S. Shresta.** 2011. Important advances in the field of anti-dengue virus research. Antivir. Chem. Chemother. **21:**105–116.
17. **Kelly, E. P., B. Puri, W. Sun, and B. Falgout.** 2010. Identification of mutations in a candidate dengue 4 vaccine strain 341750 PDK20 and construction of a full-length cDNA clone of the PDK20 vaccine candidate. Vaccine **28:**3030–3037.
18. **Kuhn, R. J., et al.** 2002. Structure of dengue virus: implications for flavivirus organization, maturation, and fusion. Cell **108:**717–725.
19. **Laurent-Rolle, M., et al.** 2010. The NS5 protein of the virulent West Nile virus NY99 strain is a potent antagonist of type I interferon-mediated JAK-STAT signaling. J. Virol. **84:**3503–3515.
20. **Leardkamolkarn, V., W. Sirigulpanit, and R. M. Kinney.** 22 March 2010. Characterization of recombinant dengue-2 virus derived from a single nucleotide substitution in the 5′ noncoding region. J. Biomed. Biotechnol. doi:10.1155/2010/934694.
21. **Lee, K. S., et al.** 2010. Dengue virus surveillance for early warning, Singapore. Emerg. Infect. Dis. **16:**847–849.
22. **Leitmeyer, K. C., et al.** 1999. Dengue virus structural differences that correlate with pathogenesis. J. Virol. **73:**4738–4747.
23. **Libraty, D. H., et al.** 2002. High circulating levels of the dengue virus nonstructural protein NS1 early in dengue illness correlate with the development of dengue hemorrhagic fever. J. Infect. Dis. **185:**1213–1221.
24. **Lindenbach, B. D., H.-J. Thiel, and C. M. Rice.** 2007. *Flaviviridae*: the viruses and their replication, p. 1101–1152. *In* D. M. Knipe et al. (ed.), Fields virology, 5th ed., vol. 1. Lippincott Williams & Wilkins, Philadelphia, PA.
25. **Liu, W., et al.** 2005. Inhibition of interferon signaling by the New York 99 strain and Kunjin subtype of West Nile virus involves blockage of STAT1 and STAT2 activation by nonstructural proteins. J. Virol. **79:**1934–1942.
26. **Lo, L., M. Tilgner, K. Bernard, and P.-Y. Shi.** 2003. Functional analysis of mosquito-borne flavivirus conserved sequence elements within 3′ untranslated region of West Nile virus by use of a reporting replicon that differentiates between viral translation and RNA replication. J. Virol. **77:**10004–10014.
27. **Messer, W. B., et al.** 2002. Epidemiology of dengue in Sri Lanka before and after the emergence of epidemic dengue hemorrhagic fever. Am. J. Trop. Med. Hyg. **66:**765–773.
28. **Miller, S., S. Sparacio, and R. Bartenschlager.** 2006. Subcellular localization and membrane topology of the dengue virus type 2 non-structural protein 4B. J. Biol. Chem. **281:**8854–8863.
29. **Muñoz-Jordan, J. L., et al.** 2005. Inhibition of alpha/beta interferon signaling by the NS4B protein of flaviviruses. J. Virol. **79:**8004–8013.
30. **Muñoz-Jordan, J. L., G. G. Sanchez-Burgos, M. Laurent-Rolle, and A. Garcia-Sastre.** 2003. Inhibition of interferon signaling by dengue virus. Proc. Natl. Acad. Sci. U. S. A. **100:**14333–14338.
31. **Noble, C. G., et al.** 2010. Strategies for development of dengue virus inhibitors. Antiviral Res. **85:**450–462.
32. **Pandey, B. D., K. Morita, F. Hasebe, M. C. Parquet, and A. Igarashi.** 2000. Molecular evolution, distribution and genetic relationship among the dengue 2 viruses isolated from different clinical severity. Southeast Asian J. Trop. Med. Public Health **31:**266–272.
33. **Prestwood, T. R., D. M. Prigozhin, K. L. Sharar, R. M. Zellweger, and S. Shresta.** 2008. A mouse-passaged dengue virus strain with reduced affinity for heparan sulfate causes severe disease in mice by establishing increased systemic viral loads. J. Virol. **82:**8411–8421.
34. **Proutski, V., T. S. Gritsun, E. A. Gould, and E. C. Holmes.** 1999. Biological consequences of deletions within the 3′-untranslated region of flaviviruses may be due to rearrangements of RNA secondary structure. Virus Res. **64:**107–123.
35. **Qing, M., et al.** 2010. Characterization of dengue virus resistance to brequinar in cell culture. Antimicrob. Agents Chemother. **54:**3686–3695.
36. **Rosen, L.** 1977. The Emperor's New Clothes revisited, or reflections on the pathogenesis of dengue hemorrhagic fever. Am. J. Trop. Med. Hyg. **26:**337–343.
37. **Sánchez, I. J., and B. H. Ruiz.** 1996. A single nucleotide change in the E protein gene of dengue virus 2 Mexican strain affects neurovirulence in mice. J. Gen. Virol. **77:**2541–2545.
38. **Steel, A., D. J. Gubler, and S. N. Bennett.** 2010. Natural attenuation of dengue virus type-2 after a series of island outbreaks: a retrospective phylogenetic study of events in the South Pacific three decades ago. Virology **405:**505–512.
39. **Tan, G. K., et al.** 2010. A non mouse-adapted dengue virus strain as a new model of severe dengue infection in AG129 mice. PLoS Negl. Trop. Dis. **4:**e672.
40. **Tang, Y., et al.** 2010. Both viremia and cytokine levels associate with the lack of severe disease in secondary dengue 1 infection among adult Chinese patients. PLoS One **5:**e15631.
41. **Trung, D. T., and B. Wills.** 2010. Systemic vascular leakage associated with dengue infections—the clinical perspective. Curr. Top. Microbiol. Immunol. **338:**57–66.
42. **Umareddy, I., A. Chao, A. Sampath, F. Gu, and S. G. Vasudevan.** 2006. Dengue virus NS4B interacts with NS3 and dissociates it from single-stranded RNA. J. Gen. Virol. **87:**2605–2614.
43. **Vaughn, D. W., et al.** 2000. Dengue viremia titer, antibody response pattern, and virus serotype correlate with disease severity. J. Infect. Dis. **181:**2–9.
44. **Vu, T. T., et al.** 2010. Emergence of the Asian 1 genotype of dengue virus serotype 2 in Viet Nam: *in vivo* fitness advantage and lineage replacement in South-East Asia. PLoS Negl. Trop. Dis. **4:**e757.
45. **Watts, D. M., et al.** 1999. Failure of secondary infection with American genotype dengue 2 to cause dengue haemorrhagic fever. Lancet **354:**1431–1434.
46. **Whitehead, S. S., et al.** 2003. A live, attenuated dengue virus type 1 vaccine candidate with a 30-nucleotide deletion in the 3′ untranslated region is highly attenuated and immunogenic in monkeys. J. Virol. **77:**1653–1657.